地学雑誌　Journal of Geography（Chigaku Zasshi）　134（6）615–624 2025　doi:10.5026/jgeography.134.615

First Muography of Samail Ophiolite at Wadi Fizh

László OLÁH[1) 2)], Susumu UMINO[3)], Yuki KUSANO[4)], Tomoaki MORISHITA[3)], Said Mohammed AL MUSHARRAFI[5)], Nasser Saif Said AL MAAWALI[5)], Ibrahim Awadh Mohammed AL SAWAFI[5)], Hiroyuki K. M. TANAKA[1) 6)], László TERCSI[2)] and Dezső VARGA[1) 2)]

［Received 2 September, 2024; Accepted 6 January, 2025］

Abstract

Ophiolites provide useful information about the evolution of oceanic lithosphere that has not yet been assessed by drilling experiments to date. In spite of the relevance of ophiolites, geophysical explorations provided sparse data about the internal structure of these natural formations. We propose a novel geophysical technique, called muography, that allows scanning of the internal density structure of ophiolites by measuring the yield of naturally occurring cosmic-ray muon particles which penetrate across the ophiolites. We report on the first muographic experiment that is in progress to image the mass density structure of an ophiolite segment at Wadi Fizh in the Samail ophiolite, Sultanate of Oman. The installation and commissioning of the experimental setup, the operational performance of the muographic observation system and the preliminary results are presented. The structure of lower crust can be distinguished from the upper mantle and Moho transition zone in a preliminary mass density image. Data collection will be continued at the current position and at additional measurement sites around the ophiolite segment to resolve its density structure in three dimensions with sufficient spatial and density resolution for studying the Moho transition zone.

Key words：cosmic-ray muons, muography, oceanic lithosphere, moho, ophiolite

I. Introduction

Lithosphere is built up from the crust and solid upper mantle beneath lands and waters（Koppers and Coggon, 2020）. Cycling of materials and energy in the lithosphere influences Earth's sub-systems（e.g., produces natural resources, triggers natural disasters, etc.）. Seismic measurements revealed transition zones between the upper and lower crust as well as between the lower crust and the upper mantle. The latter transition zone is the so called Mohorovičić discontinuity zone, shortly Moho. It is challenging to reach the Moho because it is located 5–6 km beneath seabeds and 25–30 km beneath the continents. Oceanic drilling experiments are being under development to explore the relatively thinner oceanic lithosphere（e.g., Karson, 2002; Swift *et al*., 2008; Umino *et al*., 2013）but researchers are still lack of samples

[1)] International Virtual Muography Institute, Tokyo, 113-0032, Japan
[2)] Institute for Particle and Nuclear Physics, HUN-REN Wigner Research Centre for Physics, Budapest, 1121, Hungary
[3)] College of Science and Engineering, Kanazawa University, Kanazawa, 920-1164, Japan
[4)] Geological Survey of Japan, Tsukuba, 305-8561, Japan
[5)] Ministry of Energy and Minerals, Muscat, 113, Sultanate of Oman
[6)] Earthquake Research Institute, The University of Tokyo, Tokyo, 113-0032, Japan

from the Moho. To date the physical nature and geological meaning of the transition zones remain poorly understood. The oceanic Moho shows a variety of seismic structures from multiple reflections, sharp single reflections, diffused reflections, and no reflections (Ohira *et al.*, 2017). In the Samail Ophiolite, the Moho comprises a lithological transition zone of alternating layers of dunite and gabbro between crustal gabbro and mantle harzburgite, which is thickest in the center of the paleoridge segment and thinnest at the ends (Oláh *et al.*, 2024). These intrasegment variations of the Moho transition zone may result in different seismic reflections that explain the diversity of the oceanic Moho. Studying ophiolites provides opportunities to learn about the nature of oceanic lithosphere because these structures incorporate the obducted fragments of lithosphere formed via the evolution of mid-ocean ridges. The Samail Ophiolite is one of the most complete analogues for the oceanic lithosphere (Searle and Cox, 1999), however sparse data have been provided by geophysical techniques about its internal structure to date.

We aim to utilize a novel geophysical imaging technique called cosmic-ray muography (Oláh *et al.*, 2024) for exploring the different stratigraphic layers in the Samail Ophiolite. This passive, non-destructive and remote technique allows to explore the mass density structure of solid, liquid and gaseous materials (Oláh *et al.*, 2022; Tanaka *et al.*, 2023). The omnipresence, approximately stationary yield and small interaction cross section of cosmic-ray muons allow them to penetrate across large volumes (even a few cubic kilometres) of rocks with negligible deflections. Consequently, muography can provide density information with relatively high spatial resolution (even with a resolution of a few metres) from volumes that have limited accessibility for other geophysical techniques, such as electrical resistivity tomography or gravimetric surveys.

Plans for a muography campaign in the Samail Ophiolite have already been proposed and presented in Ref. (Oláh *et al.*, 2024). Different sites are under investigation. Figure 1A and 1B highlight two candidate ophiolite segments that include transition zones between the upper and lower crust layers at Wadi Halti (A) and between the lower crust and upper mantle at Wadi Fizh (B). In this work, we present a pilot muography measurement that has already been started at Wadi Fizh.

II. Experimental setup

A 60-km long paleoridge segment has been defined in the northern Oman Mountains by structural and geochemical studies (Adachi and Miyashita, 2003; Miyashita *et al.*, 2003; Umino *et al.*, 2003; Oláh *et al.*, 2024). We decided to study the structural differences between the thick and thin Moho transition zones in this paleoridge segment. We chose the thin Moho transition zone of Wadi Fizh (Fig. 1B) as our first target for the segment end. In addition to its geological importance, the site was chosen because of technical constraints such as accessibility by car and availability of electricity, the thickness of the rock (several hundred meters) measurable by the muography, and the absence of an obstructing ridge behind the target. The goals of the first data collection campaign are the following: (1) Testing and optimizing the muographic observation system (MOS) in the harsh and varying environment. (2) Muographic mass density imaging the Moho transition zone located between the lower crust and the upper mantle.

Figure 2 presents the first experimental arrangement at Wadi Fizh. We installed a Multi-Wire-Proportional-Chamber (MWPC)-based Muographic Observation System (MMOS) in a plastic hut at a latitude of 24.45655 deg N and a longitude of 56.29703 deg E and an altitude above sea level of 465 m about a distance of 300 m from the ophiolite (red coloured x in Fig. 2A). The MMOS was oriented to an azimuthal direction of 298 deg from north (red arrow in Fig. 2A) to observe the Moho region with maximum detector acceptance. It is important to emphasize that it was not possible to install the detector closer to the ophiolite due to the

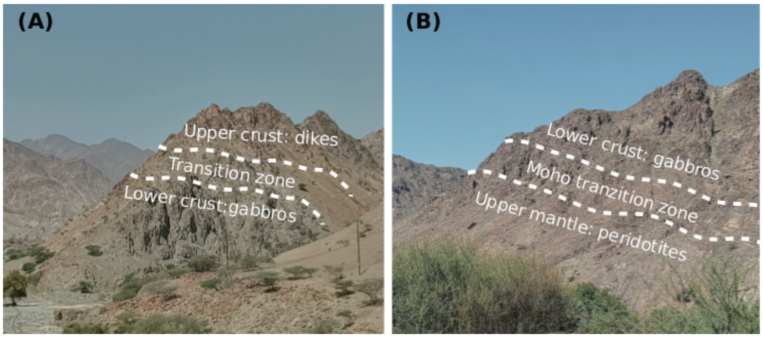

Fig. 1 Photographs of crustal and mantle layers of the Samail Ophiolite. (A) The upper and lower crustal boundaries are respectively built up from dikes and gabbros at Wadi Halti. (B) The Moho transition zone is located between gabbros and peridotites at Wadi Fizh.

presence of a river bed along the foot of the ophiolite and the corresponding risk of flooding. Figure 2B shows a photograph of the hut and its surroundings including the studied ophiolite segment in the background. Figure 2C visualizes the calculated path-lengths of cosmic-ray muons across a selected region (black rectangle of Fig. 2B) in the coordinate system of MMOS that is based on the horizontal- and elevation slopes (tangents of horizontal- and vertical angles) of muon trajectories. These angular bins have a size of 0.016 × 0.016. This angular bin size was chosen to have sufficient statistics (a few tens of muon tracks) in each angular bin across the transition zone to calculate the mass densities. This angular bin corresponds to pixels with an area of 4.8 m × 4.8 m across the ophiolite located at a distance of 300 m. This angular binning is used in the remaining figures.

Figure 3 shows a photograph of the experimental apparatus. The MWPC technology and MMOS are presented extensively in Refs. (Varga *et al*., 2016; Oláh *et al*., 2018). This muon tracking system has been built up from seven MWPCs with a surface area of 80 cm × 80 cm and thickness of 2 cm each and two lead walls with the same surface area and a thickness of 2 cm each along the length of 150 cm.

The MWPCs are gaseous particle detectors that are applied for measuring the trajectories of charged particles which penetrate across their sensitive volumes (Varga *et al*., 2016).

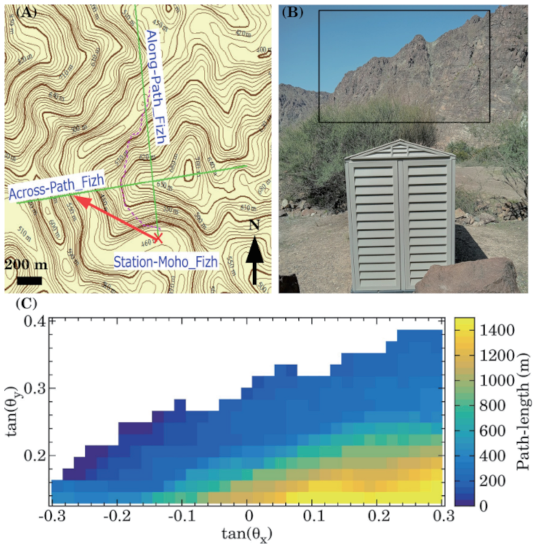

Fig. 2 The experimental setting at Wadi Fizh in the Samail Ophiolite. (A) Map of measurement site in which red “x” indicates the location of muographic observation system (MOS) at latitude of 24.45655 deg Northing and longitude of 56.29703 deg Easting and altitude of 465 m above sea level. The azimuthal orientation of MOS was set to 298 deg from north as shown by a red arrow. (B) A photograph of detector housing with the ophiolite to be imaged in the background. (C) Path-lengths of muons across the studied region (black rectangle in Fig. 2B) are shown as a function of horizontal and elevation slopes (tangents of horizontal- and vertical angles).

Fig. 3　A photograph of the muographic observation system with its gas system and power supply system.

MWPCs utilize a series of wires in a closed gas volume for production of electric signals. In our MWPCs two perpendicular wire planes are applied each with a wire spacing of 12 mm. This wire spacing allows the localization of particles' positions with a resolution of approx. 4 mm. An environmentally friendly (non-flammable and non-toxic) industrial gas mixture with Ar (volume fraction of 0.8) and CO_2 (volume fraction of 0.2) gases is flushed across the MWPCs for signal production. The electrons are created via ionization of gas atoms by the charged particles that penetrate across the gas volume. Typically 200 electrons are created in the gas mixture. A high-voltage of about 1.7 kV is applied on the anode wires to gain the number of electrons to a few thousands via avalanche process. The electrons are collected on the wires and their signal is amplified by a factor of 10 and discriminated by custom designed front-end cards.

A microcomputer-based detector control and data acquisition (DAQ) system is applied in the MMOS (Varga *et al.*, 2016). A custom designed temperature-humidity-pressure (THP) sensor monitors these parameters during operation. Data are collected on an event-by-event basis. Each event is built up from the following data: a time stamp, a time in microseconds passed since the time of the previous event, particles' hits on MWPCs, analogue signal amplitudes, trigger bits, THP values and high-voltage values. The data collection is triggered by the triple coincidence of MWPCs, i.e. when at least three MWPCs detected the particle at the same (within a few microseconds) time. The acquired data is written into ASCII files on an event-by-event basis. The trigger is blocked during the data readout which results in a dead time of 100 microseconds for each event. This dead time results in a loss of muons below 0.1%.

The lead plates are applied to absorb and deflect the low-momenta muons and other charged particles (Nishiyama *et al.*, 2016) that are observed from the direction of ophiolite but did not penetrate across it. These are mostly low-momentum particles which suffer small deflections along their paths in the lead walls due to their electromagnetic interactions with the lead atoms. These multiple scatterings result in spatial displacements that are inversely proportional to particles' momenta. These particles do not create straight trajectories in the tracking system and can be removed from the track set before muon imaging by applying an analysis cut on the goodness of the line fit (Oláh *et al.*, 2018).

The detector installation and commissioning have been conducted between 25–27 February 2024. Gas supplying is provided by a 40 L volume gas cylinder that is filled with a pressure of 140 bar. Such volume allows a continuous operation of 3–4 month with a gas flow of 2–3 Liters per hour. Power supply has been provided by the local electricity network. We note that it is possible to operate the MMOS using batteries and solar panels, however testing of the latter could not be completed due to limited time available for installation work. Currently only the gas supplying limits the duration of detector operation. It is important to highlight that all elements of the MMOS are based on materials that pose no risk of damage to nature.

III. Data collection and processing

The data collection was started on 28 February 2024. The experimental site has been visit-

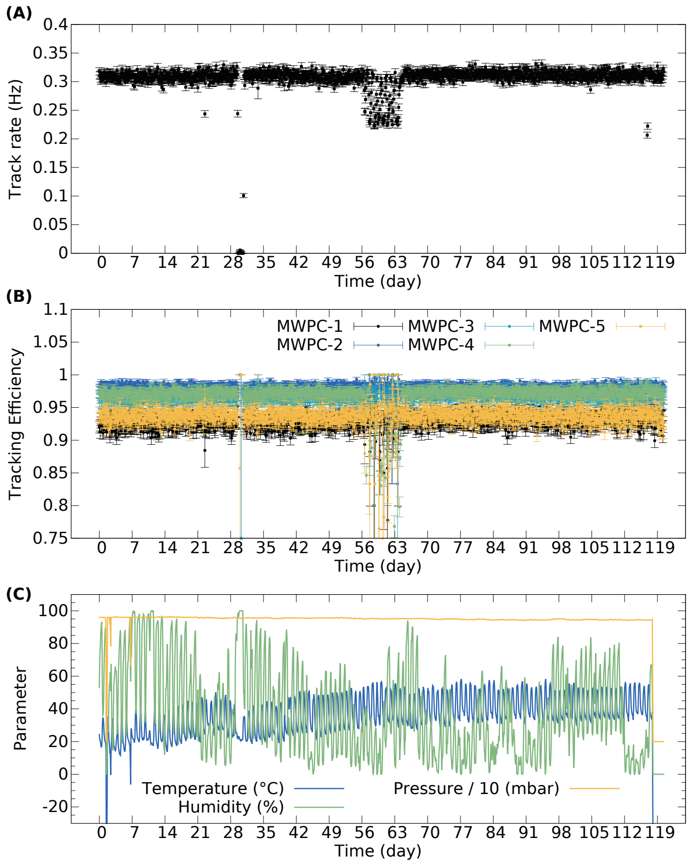

Fig. 4 The time-line of (A) track rates, (B) tracking efficiencies and (C) environmental parameters are shown with a time binning of 2 hours during the date collection period, which started on 27 February, 2024.

ed by a local collaborator every 3–4 weeks who downloaded the data and conducted the maintenance of power supply system if it was necessary. The gas bottle was replaced in June. The microcomputer-based DAQ allows remote control and access, however the mountainous area did not allow to remote access to the tracking system during its operation because the mountains shielding the telephone network. Thus we performed the analysis offline.

An event-by-event procedure has been applied for data reconstruction and analysis. The methods have already been presented in Ref. (Oláh *et al.*, 2018). In a nutshell, this procedure reconstructs the clusters of particle hits, conducts combinatorial track reconstruction to determine the parameters (the slopes that are tangents of vertical- and horizontal angles, the intercepts and the chi-square per number of degrees of freedom, where the chi-square is the sum of the squares of distances between the hit cluster centroids and fitted line coordinates and the number of degrees of freedom equals to the number of MWPCs minus two) for the optimally fitting lines. The data of five MWPCs have been used for this study due to the malfunctioning of two detector layers.

Figures 4A–C present the variations in the performance of the five MWPCs and environmental parameters with a time bin size of 2 hours for the data collection period from 28 February to 1 August 2024. The track rate (Fig. 4A) is measured around 0.3 Hz with variations of a few percentages during the data collec-

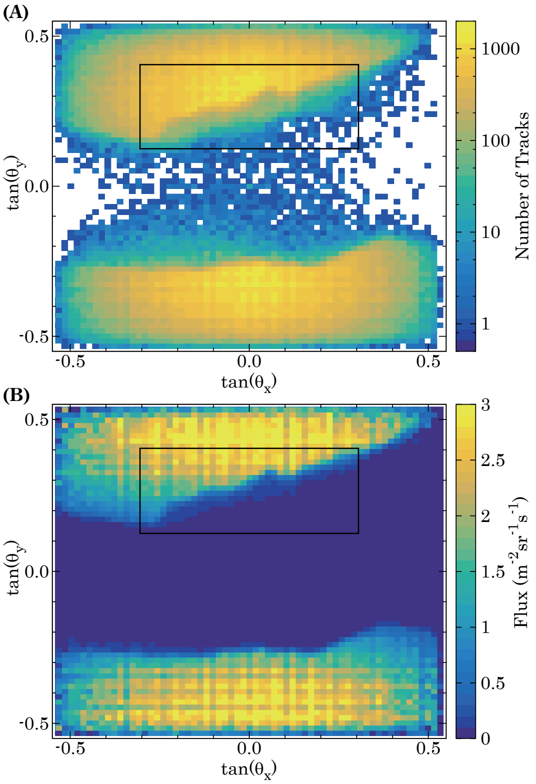

Fig. 5 Directional dependent detection of cosmic-ray muons. The number of tracks (A) and the corresponding flux (B) are shown as a function of horizontal- and elevation track slopes. Black rectangles highlight the studied region of the ophiolite.

tion period mainly due to atmospheric pressure changes. Two exceptions are observed for days 29–30 and days 57–64 when electronics noise caused temporary decreases in the track rate. The tracking efficiencies (Fig. 4B) have been measured above 90% for each MWPC except for the aforementioned periods.

Each angular dependent quantity was measured in the "natural" coordinate system of the MMOS that is based on the track slopes. Figures 5A–B respectively show the number of tracks (N) and flux (F). The flux value is determined for each angular bin by the following expression:

$$F = N/(A \times \Omega \times T) \tag{1}$$

where tracks with a $\chi^2/ndf < 1$ are selected to count N, A is the surface area, Ω is the solid angle and T is the measurement time. Both track count and flux values reflect the shape of the ridge of the ophiolite and local topography. The black rectangles (see also in Fig. 2B) highlight the region of interest.

Density-lengths were determined by means of comparing the measured fluxes (Fig. 5B) to calculated fluxes determined for different density-lengths. The density-lengths were extracted when the difference between the measured and calculated fluxes were minimal. Errors of density-lengths were calculated via the same procedure, but the measured flux errors were added to the measured fluxes to quantify the lower density-length errors and were subtracted from the measured fluxes to determine the upper density-length errors. The calculated fluxes were determined by integrating the zenith-angle dependent muon momentum spectra (Tang *et al.*, 2006) from minimum energies that are required for muons to penetrate across a given density-length (Groom *et al.*, 2002). Figure 6 shows the calculated fluxes for different elevation angles and measured vertical muon flux data (Miyake *et al.*, 1964; Castagnoli *et al.*, 1965; Crouch, 1987). The calculated fluxes are consistent with the measured fluxes that validates our calculation method. Further validation of the muon flux calculation method has been presented in Ref. (Oláh *et al.*, 2018).

Figures 7A–B respectively show the extracted values of density-length and average values of upper and lower density-length errors as a function of track slopes. These show the amount of materials across the ophiolite segment. The mass densities have also been determined via dividing the density-lengths with the path-lengths (Fig. 2C).

IV. Preliminary results

Figure 8 shows a preliminary muographic mass density image of the ophiolite segment at Wadi Fizh. The white-shaded regions without average density values are due to the lack of

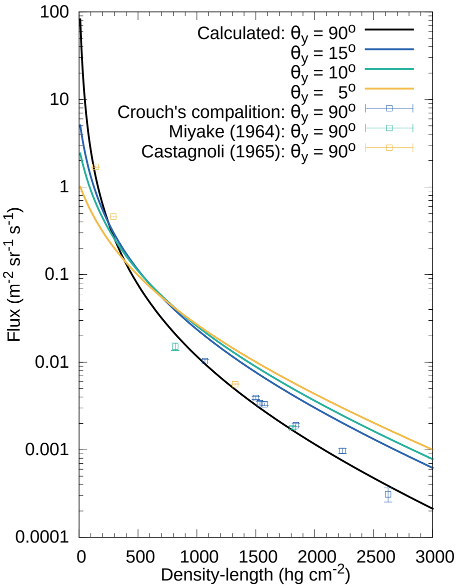

Fig. 6　Examples for calculated fluxes versus density-length are shown for selected elevation angles. To validate the calculation, we show the comparison of calculated vertical fluxes and measured vertical fluxes (Miyake *et al.*, 1964; Castagnoli *et al.*, 1965; Crouch, 1987).

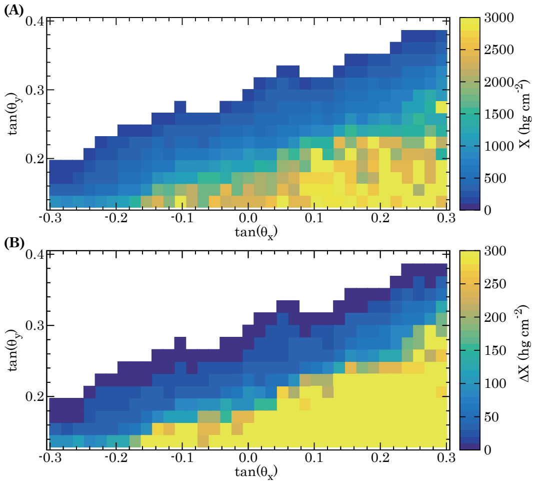

Fig. 7　The density-lengths (X) measured by cosmic-ray muography. (A) The density-lengths are plotted for the selected region (black rectangle in Fig. 5) as a function of horizontal- and elevation track slopes. (B) The averaged density-length errors are shown for the same region.

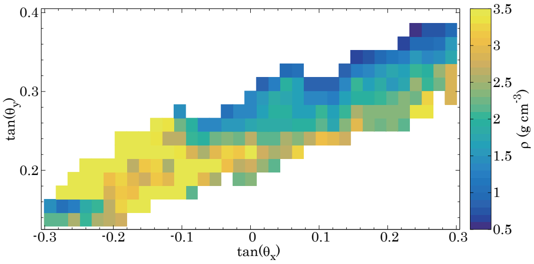

Fig. 8　The mass density values determined along the muon paths are shown as a function of horizontal- and elevation track slopes.

solid materials above the mountain ridge and the large thicknesses (Fig. 2C) that are not yet penetrated across sufficient number of muons. Across the ophiolite, two regions are clearly distinguished: (1) a low-density region above the elevation slope of 0.24 in which the values measured from 0.5 g cm^{-3} to 3 g cm^{-3} and (2) a high-density regions below the elevation slope of 0.24 in which the values are measured above 3 g cm^{-3}. The density region (1) corresponds to the gabbros of the lower crust. The density region (2) corresponds to the rock of Moho and peridotites of the upper mantle. The currently available data and methodology do not allow us to distinguish the Moho from the upper mantle.

V. Summary and outlook

Studying the mass density structure of ophiolites can provide information about the nature of oceanic Moho. Muography allows passive, remote and non-destructive exploration of the internal density structure of ophiolites by measuring the naturally occurring cosmic-ray muon particles using sustainable and environmentally friendly detector technology. We have successfully launched the first muography campaign at Wadi Fizh in the Samail ophiolite. The muography observation instrument has already accumulated good quality data over 4 months in the harsh and varying environment. The first muographic density image has been determined with a pixel size that corresponds to a spatial resolution of 4.8 metres in the ophiolite. We could distinguish the Moho and upper mantle from the lower crust.

The angular resolution of MMOS would allow reduction of the spatial resolution from 4.8 m to 1.2 m even at the current location, however it would require longer data collection period due to the limited yield of muons. In future work, we plan to apply larger muographic data sets collected at the Moho transition zone in the center of the paleoridge segment located closer to the ophiolite to reconstruct the mass density distribution in 3 dimensions with higher spatial resolution and explore the structure and constitution of the boundary between the Moho from the upper mantle. Such precise density data may allow us (1) to explore the diversity of Moho along the paleoridge segment in both vertically and laterally and (2) to reveal whether the discontinuity forms either sharp or multiple seismic reflections. These may allow us to infer to the physical processes that occurred between the diverse oceanic Moho.

Acknowledgements

This project is supported by the ERI JURP 2023-H-01, 2023-H-03 and 2024-H-01 grants of Earthquake Research Institute, the University of Tokyo, MEXT Grant-in-Aid for Scientific Research (KAKENHI) under project ID 24K00731 and HUN-REN Welcome Home and Foreign Researcher Recruitment Programme KSZF-144/2023. Instrumentation is constructed in the Vesztergombi Laboratory for High Energy Physics (VLAB) with the support of Hungarian NKFIH research grant under identification number TKP2021-NKTA-10.

References

Adachi, Y. and Miyashita, S. (2003): Geology and petrology of the plutonic complexes in the Wadi Fizh area: Multiple magmatic events and segment structure in the northern Oman ophiolite. *Geochemistry, Geophysics, Geosystems*, **4**, 8619, doi:10.1029/2001GC000272.

Castagnoli, C., De Marco, A., Longhetto, A. and Penengo, P. (1965): Measurements on the cosmic radiation intensity in the Mont Blanc Tunnel. *Nuovo Cimento*, **35**, 969–976.

Crouch, M. (1987): An improved world survey expression for cosmic ray vertical intensity vs. depth in standard rock. *Proceedings of ICRC 1987*, **6**, 165C.

Groom, D.E., Mokhov, N.V. and Striganov, S.I. (2002): Muon stopping power and range tables 10 MeV–100 TeV. *Atomic Data and Nuclear Data Tables*, **76**, 183–356.

Karson, J.A. (2002): Geological structure of the uppermost oceanic crust created at fast- to intermediate-rate spreading centers. *Annual Review of Earth and Planetary Sciences*, **30**, 347–384.

Koppers, A.A.P. and Coggon, R. (2020): *Exploring Earth by Scientific Ocean Drilling: 2050 Science Framework*, 124p, doi:10.6075/J0W66J9H.

Miyake, S., Narasimham, V.S. and Ramana Murthy, P.V. (1964): Cosmic-ray intensity measurements deep undergound at depths of (800 ÷ 8400) m w.e.. *Nuovo Cimento*, **32**, 1505–1523.

Miyashita, S., Adachi, Y. and Umino, S. (2003): Along axis magmatic system in the northern Oman Ophiolite: Implications of compositional variation of the sheeted dike complex. *Geochemistry, Geophysics, Geosystems*, **4**, 8617, doi:10.1029/2001GC000235.

Nishiyama, R., Taketa, A., Miyamoto, S. and Kasahara, K. (2016): Monte Carlo simulation for background study of geophysical inspection with cosmic-ray muons. *Geophysical Journal International*, **206**, 1039–1050.

Ohira, A., Kodaira, S., Nakamura, Y., Fujie, G., Arai, R. and Miura, S. (2017): Structural variation of the oceanic Moho in the Pacific plate revealed by active-source seismic data. *Earth and Planetary Science Letters*, **476**, 111–121, doi:10.1016/j.epsl.2017.08.004.

Oláh, L., Tanaka, H.K.M., Ohminato, T. and Varga, D. (2018): High-definition and low-noisy muography of Sakurajima volcano with gaseous tracking detectors. *Scientific Reports*, **8**, 3207.

Oláh, L., Tanaka, H.K.M. and Varga, D. (2022): *Muography: Exploring Earth's Subsurface with Elementary Particles. Geophysical Monograph*, American Geophysical Union, John Wiley & Sons, **270**.

Oláh, L., Umino, S., Kusano, Y., Morishita, T., Al Musharrafi, S.M., Al Sawafi, I., Tanaka, H.K.M. and Varga, D. (2024): Plans for Muography of Samail Ophiolite. *Journal of Advanced Instrumentation in Science*, **2024**, 499.

Searle, M. and Cox, J. (1999): Tectonic setting, origin, and obduction of the Oman ophiolite. *GSA Bulletin*, **111**, 104.

Swift, S., Reichow, M., Tikku, A., Tominaga, M. and Gilbert, L. (2008): Velocity structure of upper ocean crust at Ocean Drilling Program Site 1256. *Geochemistry, Geophysics, Geosystems*, **9**, Q10O13.

Tanaka, H.K.M., Bozza, C., Bross, A., Cantoni, E., Catalano, O., Cerretto, G., Giammanco, A., Gluyas, J., Gnesi, I., Holma, M., Kin, T., Lázaro Roche, I., Leone, G., Liu, Z., Lo Presti, D., Marteau, J., Matsushima, J., Oláh, L., Polukhina, N., Ramakrishna, S.S.V.S., Sellone, M., Hideki Shinohara, A., Steigerwald, S., Sumiya, K., Thompson, L., Tioukov, V., Yokota, Y. and Varga, D. (2023): Muography.

Nature Reviews Methods Primers, **3**, 88.
Tang, A., Horton-Smith, G., Kudryavtsev, V.A. and Tonazzo, A. (2006): Muon simulations for Super-Kamiokande, KamLAND, and CHOOZ. *Physical Review D*, **74**, 053007.
Umino, S., Miyashita, S., Hotta, F. and Adachi, Y. (2003): Along-strike variation of the sheeted dike complex in the Oman Ophiolite: Insights into sub-axial ridge segment structures and magma plumbing system. *Geochemistry, Geophysics, Geosystems*, **4**, 8618, doi:10.1029/2001GC000233.
Umino, S., Nealson, K. and Wood, B. (2013): Drilling to Earth's mantle. *Physics Today*, **66**, 36–41.
Varga, D., Hamar, G., Nyitrai, G. and Oláh, L. (2016): High efficiency gaseous tracking detectors for cosmic muon radiography. *Advances in High Energy Physics*, **2016**, 1962317.

ワジ・フィズ地域における
サマイル・オフィオライトの初のミュオグラフィ観測

László OLÁH [1) 2)]　海　野　　進 [3)]　草　野　有　紀 [4)]
森　下　知　晃 [3)]　Said Mohammed AL MUSHARRAFI [5)]
Nasser Saif Said AL MAAWALI [5)]　Ibrahim Awadh Mohammed AL SAWAFI [5)]
田　中　宏　幸 [1) 6)]　László TERCSI [2)]　Dezső VARGA [1) 2)]

オフィオライトは，掘削実験ではまだ十分に解明されていない海洋リソスフェアの進化に関する有益な情報を提供する。しかしながら，その重要性にもかかわらず，従来の地球物理探査手法では，オフィオライトの内部構造に関する情報は限定的であった。本研究では，宇宙線ミュオンの通過量を測定することにより，オフィオライトの内部密度構造を可視化する新たな地球物理探査手法「ミュオグラフィ」を提案する。ここでは，オマーン国サマイル・オフィオライトのワジ・フィズ地域におけるオフィオライトセグメントの密度構造を画像化するために実施中の，初のミュオグラフィ実験について報告する。観測システムの設置・試運転，ミュオグラフィ観測装置の運用性能，ならびに予備的な観測結果について紹介する。得られた予備的な密度画像からは，下部地殻構造が上部マントルおよびモホ遷移帯と区別可能であることが示唆される。今後は現在の観測地点に加え，オフィオライトセグメント周辺の複数地点でのデータ取得を継続し，モホ遷移帯の研究に資する三次元密度構造の高解像度可視化を目指す。

キーワード：宇宙線ミュオン，ミュオグラフィ，海洋リソスフェア，モホ面，オフィオライト

1）国際バーチャル・ミュオグラフィ研究所
2）HUN-REN ウィグナー物理学研究センター
3）金沢大学理工研究域
4）産業技術総合研究所 地質調査総合センター
5）オマーン国エネルギー・鉱物省
6）東京大学地震研究所